PCCP

Accepted Manuscript

ROYAL SOCIETY OF CHEMISTRY

www.rsc.org/pccp

Journal Name

ARTICLE

What is the primary mover of water dynamics?

P. Ben Ishai[a,b,†], S. R. Tripathi[b], K. Kawase[b], A. Puzenko[a] and Yu. Feldman[a]

Received 00th January 20xx,
Accepted 00th January 20xx

DOI: 10.1039/x0xx00000x

www.rsc.org/

The H-bonded cluster structure of water still stands as a major point of debate in the science of liquids today. Much of this discussion is devoted to the understanding of its dynamic nature. This has a direct impact on deciphering the many anomalies of water, such as its exceptional heat capacity and others. Of these properties its dielectric permittivity and relaxation stand out. The argument rages as to whether the almost Debye like character of the dispersion is the result of the reorientation of an apparent dipole moment of the water cluster, or simply the cumulative effect of single water molecule reorientation. Furthermore, like many glass formers, it has a high frequency excess wing, that does not fit into the accepted models of a single relaxation time of the main peak. We present evidence that the microscopic origin of both the excess wing and the main relaxation process of pure water is the same. The origin of these two features is explored and we suggest a new paradigm for water relaxation based on the concept of a proton cascade leading to a cluster reorientation.

Keywords: Water, Dielectric Spectroscopy, THz Spectroscopy

[a] Department of Applied Physics, The Hebrew University of Jerusalem, Givat Ram, Jerusalem 91904, Israel.
[b] Graduate School of Engineering, Nagoya University, Furo-cho, Chikusa-Ku, Nagoya 464-8603, Japan.
†Corresponding author: paul.benishai@mail.huji.ac.il

Introduction

In the liquid state does a water molecule continuously rotate or does it jump between orientations? This innocuous question sits at the root of understanding much of the anomalous behavior of water behaviour in at least 64 of its properties [1–3]. Formally, a number of authors invoke continuous rotational diffusion (CRD) of the individual water molecule, albeit somewhat disturbed by the local environment [4,5]. Others have pointed to the restructuring of the water via extended large angle (ELA) jumps [1,6–8]. Neither model is adequate to explain water. It is a debate that still rages, as each position has its advantages. There is a third alternative to consider. Water molecules can spontaneously disassociate to form Hydronium and Hydroxyl ions, albeit it at rates as low as every 10^{-5} s^{-} [9]. However these long living ions are the tip of an iceberg of disassociation attempts that end in recombination and each attempt perturbs the surrounding environment. We propose that this may have a significant contribution to the dynamic relaxation of water and , hence, to some of its anomalous behaviours.

Almost all researchers will point to the spanned H-bonded network that water molecules form in the liquid state, as the source of these anomalies [3,4] and the dynamic nature of how they form and change as the key to water's behaviour. The current view of this network is one of local tetrahedral structures surrounded by a sea of H-bonded, distorted and thermally excited structures. These two populations are in a state of dynamic equilibrium and these views find credence in both Molecular Dynamic Simulations [10], studies of the OH stretching mode in FTIR Spectroscopy [11,12], X-ray emission spectroscopy and SAXS [13].

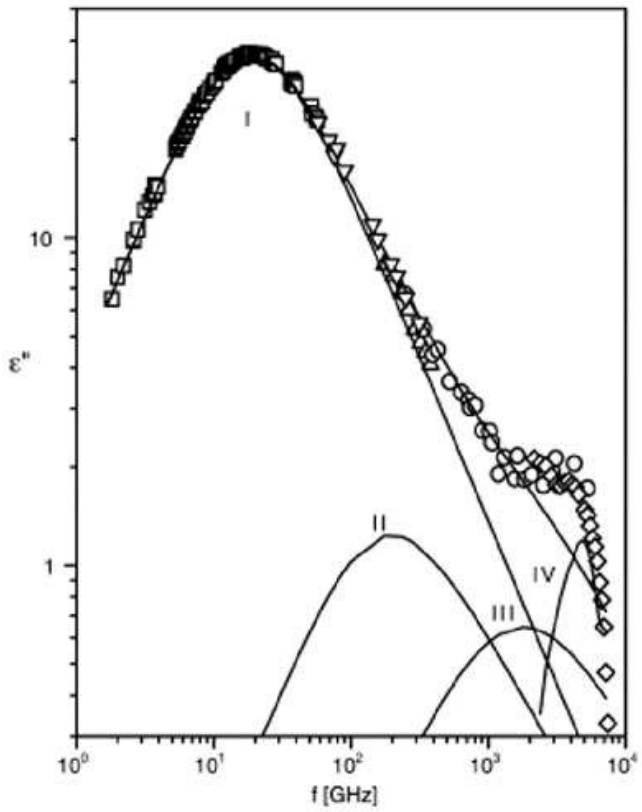

Figure 1. The dielectric losses for water at 25 C, reproduced from Vij [14]. I refers to the main dielectric peak centred around 19.3 GHz. The excess wing at frequencies higher than this main peak is clearly evident. Further relaxation terms are usually exploited to fit the wing [14] based on molecular dynamic simulations. Using molecular Dynamic simulations peak II is related to the orientation time of a single water molecule not coordinated with water clusters. Process III is associated to the vibrational relaxation of H-bonds.

These clusters can dynamically rearrange and reassemble. How this restructuring occurs is a primal question lying at the root of an understanding of water. In this paper we demonstrate that by a close examination of the dielectric permittivity of water, another of its anomalous characteristics, that the origin of water's behaviour may lie in a hitherto unrecognized mechanism based on disassociation and the concept of a proton cascade.

One of the more intriguing of water's properties is its dielectric nature. Despite possessing a dipole moment of approximately 1.8 D per molecule in the gas phase or approximately 2.7 D in the condensed phase [15–17], its dielectric properties are by no means simple [3]. A straightforward calculation reveals that the molecular dipole moment cannot account for the measured dielectric strength [3,18]. If one discounts the contribution of dc conductivity, then for frequencies up to 50 GHz the dielectric spectrum of water can be fully described by a single relaxation peak, which can be modelled adequately using the Debye formula [5,19],

$$\varepsilon^*(\omega) - \varepsilon_\infty = \frac{\Delta\varepsilon}{1+i\omega\tau} \quad , \qquad (1)$$

where $\varepsilon^*(\omega)$ is the complex dielectric permittivity, ε_∞ is the high frequency limit, $\Delta\varepsilon$ is the dielectric strength of the process, ω is the cyclic frequency and τ is the characteristic relaxation time of the process in question, 8.25 ps at 25 °C [20]. At higher frequencies one can observe an excess wing, traditionally described by the superposition of two more independent relaxation processes [14,20,21]. A typical spectrum is illustrated in figure 1, taken from Vij et al. [14]. The fitting peaks are usually associated respectively with the free rotation of uncoordinated water molecules (peak II) and with a vibrational relaxation associated with the H-bond [14] (Peak III) or possibly the libration of the water molecule [8]. Eventually vibrational modes are found around 5 THz [14] and will not be considered in this article.

Elegant as the above formula of water's dielectric response may be, this model does not predict the existence of an excess wing in its dielectric behaviour at the higher frequencies up to 2-3 THz. Other phenomenological equations prevalent in Dielectric Spectroscopy, cannot account for it either. Consequently, the wing has been modelled almost by default with further independent Debye processes [21]. Coming back to our initial question above, equation 1 can be arrived at for a single dispersion by assuming the CRD of non-interacting dipoles obeying the Fokker-Planck equation [22]. When the viscosity of water is taken into account, this approach can predict with reasonable accuracy the hydrodynamic radius of the water molecule. However, CRD cannot account for many of the anomalies of water [6,18], for instance the high specific heat of water. Furthermore, the simple cumulative effect of many water molecules independently undergoing CRD falls short of explaining the high dielectric strength of water or its relaxation time [6]. In order to square this with the measured specific heat, a strong translational element must be introduced to the picture of water reorientation [4,23]. Even so, It is still quoted by many authors in regards to dielectric relaxation [24,25]. A preferable model is championed by a number of authors [4,26–28] by which the dielectric response is derived from the apparent dipole moment of the water cluster. In this view, locally coordinated water molecules, having all 4 H-bonds occupied, can be regarded as clustered. By studying the OH stretching mode in FTIR, it appears that only about 50% of the molecules are so structured [11] in liquid water. While the average number, *N*, of water molecules in such a coordinated region is still a matter of some debate, at any time there are at least $N! - N$ combinations to arrange the individual water molecular dipoles. It is the vector sum of these molecular moments that presents an apparent dipole moment.

This is a dynamic concept, susceptible to reorganisation by the dissolving of H-bonds and reorientation of the constituent molecules. It is the cumulative reaction of these apparent moments, rather than the reorientation of uncoordinated water molecules, that leads to the large dielectric response of bulk water and the validity of Equation 1 [3].

Whether one accepts the ELA model or CRD as the molecular mechanism of water relaxation, the Excess Wing remains as an independent entity in the range of molecular motions considered. Furthermore, its role in the H-bond network is even more obscure. One could argue that this separation is also a consequence of different scientific communities – THz Spectroscopy on one hand [21,29] and Dielectric Spectroscopy on the other [3] – investigating the same material from different points of view. It is a valid question to ask if there is not a more "continuous" view of water relaxation, linking these fast and relatively slow dynamic pictures. In this work we show that the experimental evidence exists that this is indeed the case, that the main dielectric peak and the excess wing share a common molecular mechanism. Furthermore, the source of this mechanism can by rooted to fast mobilities leading to the excess wing.

Methods

The dielectric measurements of the permittivity of water up to 50 GHz were carried out in the Hebrew University, Department of Applied Physics. Triple distilled water was used with no further degassing. Measurements were carried out using a Vector Network Analyser (Agilent N5245A PNA-X) and the Agilent slim-form probe (#85070E) with their proprietary software. The calibrations used were the open line, short circuit and pure water at 25 °C.

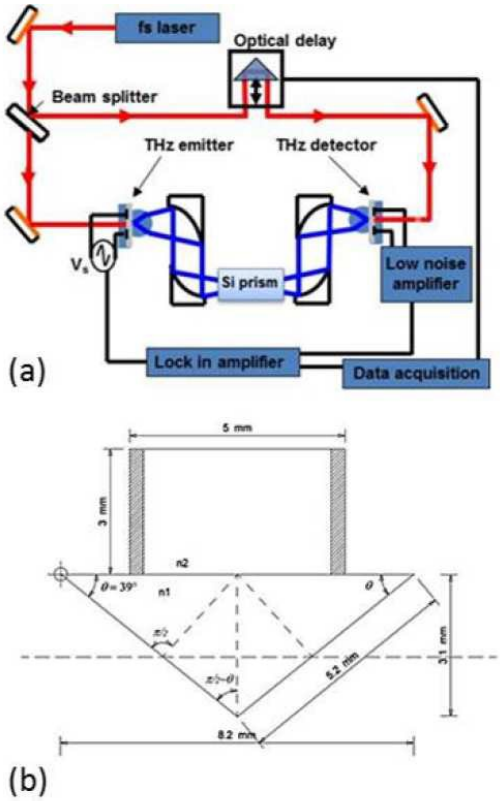

Figure 2. (a) A schematic of the TDS-THz system constructed for these measurements. The system is based on a Femtosecond pulsed laser with photoconductive antennas as both generators and detectors of THz. The setup is for transition mode and the measurements were made based on Attenuated Total Reflection (ATR), using a Si prism [30]; (b) A schematic of the prism, including the dimensions and the glass sample bath attached to the base. The indices of refraction of the prism and the sample are indicated by n_1 and n_2 respectively.

The sample holder was jacketed and thermal stabilization was maintained using a Julabo CF 41 heat circulatory system based on oil. The sample holder volume was approximately 8 ml. Measurements were carried out in the frequency range 100 MHz to 50 GHz (1021 frequency points in a log scale).

Measurements of the excess wing were made using a Time Domain Terahertz Spectroscopy (TDS-THz), which uses coherent pulse of THz waves to probe the sample under investigation. In our spectrometer, the emission and detection of coherent THz time domain pulses

were accomplished using low-temperature grown photoconductive antennas (PCA) as shown in Figure 2.

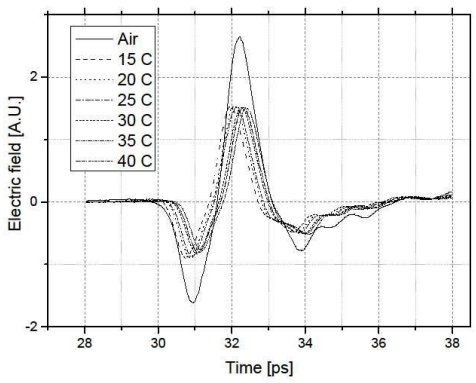

Figure 3. The measured waveforms of water as a function of temperature. The reference shown in the figure is for the empty cell at 26 C. Because the Silicon prism can act as a heat sink, the reference for each temperature was the empty cell with the prism kept at the same temperature.

Both antennas were separately excited using the femto-second fiber laser (Femtolite, IMRA Inc, HFX-400) with the wavelength = 805nm , pulse width < 80fs, repetition frequency = 67.1 MHz and variable average power = 150 mW. The basic design of a transmission TDS-THz setup is described in Figure 2a. In the focal point, we inserted the Silicon prism in order to get attenuated total reflection (ATR) of THz waves [30]. According to the dielectric properties of the sample place on the prism, the pulse is delayed and changes the pulse shape, which then finally incident on the THz detector. The frequency resolution of our THz TDS system was 25 GHz, which is sufficient to know the frequency dependent characteristics of optical constants of our sample.

Glass walls were glued to the base of the prism to create a bath 5 mm deep (see figure 2b). The temperature of the sample liquid was maintained using a stainless steel block immersed 2 mm into the water. The evanescent wave was estimated to penetrate the liquid sample no more than a few nanometers. The block was heated using a Peltier element controlled by a thermocouple. The measured waveforms are presented in Figure 3. The reflected electric field was determined by the Fourier transform of the measured waveform. The reflection coefficient was determined by comparisons of the fields of the empty bath, E', against the field of the sample; E,

$$\frac{E(\omega)}{E\prime(\omega)} = \frac{r(\omega)}{r\prime(\omega)}, \qquad (2)$$

Where r and r' are the complex reflection coefficients of the sample and the empty bath respectively. Under the condition that there is total internal reflection, the reflection coefficient, r, can be analytically written as

$$r = \frac{n_1\sqrt{1-\left(\frac{n_1}{n_2}sin\theta\right)^2}-n_2cos\theta}{n_1\sqrt{1-\left(\frac{n_1}{n_2}sin\theta\right)^2}+n_2cos\theta} \quad \text{where } n_1 > n_2 \qquad (3)$$

Where n_1 and n_2 are the indices of refraction for the prism (Silicon) and the sample respectively, and θ is the angle of the vertex. Equation 3 can be rearranged to provide an expression for the complex dielectric permittivity, $\varepsilon^*(\omega)$, of the sample,

$$\varepsilon^* = n_2^2 = n_1^2 \cdot \frac{A+\sqrt{A^2-AB\sin^2 2\theta}}{2Bcos\theta}, \qquad (4)$$

Where $A=(r-1)^2$ and $B=(r+1)^2$. While the index of refraction of silicon is constant in the THz frequency region, it is temperature dependent. Consequently, for the reference measurement for each temperature the prism was heated to the appropriate temperature.

Results

The dielectric losses for triple distilled water in the temperature range 5 °C to 70 °C and the frequency range 0.1 GHz to 1.5 THz are presented in Figure 4.

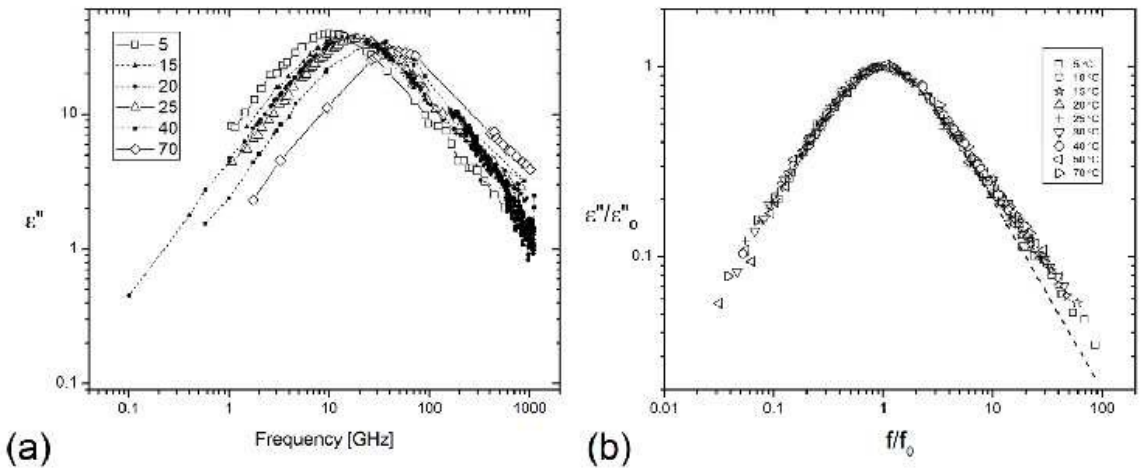

Figure 4. (a) The dielectric losses of pure water in the frequency band 0.1 GHz to 1 THz for the temperature range 5 °C to 70 °C. For the sake of clarity on the 5 temperatures are shown in the figure. The open symbols are taken from Ellison [31] and the solid symbols are the experimental results of this work. The lines are for the convenience of the reader. (b) The same data normalized in a master plot, whereby for each temperature the spectrum is normalized by the amplitude of the main dielectric peak and the frequency scale by the characteristic of the same peak. The temperature scans collapse to the same curve in this representation. The dashed line is the Debye fit for the main water dispersion peak and emphasises the existence of an excess wing feature.

While the measurements of this paper were made between 15 °C to 40 °C the data in Figure 4 have been augmented by data taken from literature [31,32] to extend the range of spectra from 5 °C to 70 °C. The main feature is a strong dielectric relaxation peak, conforming to a Debye function (equation 1). The peak frequency demonstrates an Arrhenius dependence on temperature [3] with an activation energy of 23 kJmol^{-1}. At 25 °C the peak frequency is in the region of 19.3 GHz. As the frequency is increased it is apparent that the data diverges from the Debye model of dielectric relaxation to reveal the existence of a distinct excess wing.

In order to explore the connection between the main dielectric peak and the excess wing, one can employ a simple phenomenological technique known as a master plot. For each temperature, the measured spectrum is normalised by the amplitude of the dominant feature, in this case the main Debye relaxation peak of water (Figure 4(a)), and the frequency scale is normalized by the peak frequency of the same feature. This allows all the temperature based spectrums to be displayed on the same graph. Any anomalies in the ensuing curves point to a difference of thermal behaviour, for that frequency range, from the main dielectric relaxation and probably point to the existence of a separate relaxation. Surprisingly for the temperatures 5 °C – 70 °C all relaxation curves collapse to a common curve in

the frequency band up to 2 THz. The master plot for temperatures from 5 °C to 70 °C is illustrated in Figure 4(b). As a reference, the common Debye fit (equation 1) is plotted on the same graph as a dashed line.

Discussion

The implication for a collapse of all temperature slices to a single curve in the master plot representation is that the main peak and the excess wing of the dielectric spectrum share the same thermal origin and the same energy of activation. This stands in contrast to the various models, based on the multiple Debye fits [14,29,33] and molecular dynamic simulation [21],. Obviously, the excess wing relates to mobilities faster than characteristic time for the reorganization of the main water cluster (8.28 ps at 25 °C). Consequently, as the frequency is increased, these elements of the relaxation mechanism dominate. Phenomenologically, this can be described by a modification to the dielectric strength at frequencies higher than the main peak frequency. A similar idea has been proposed before for water/glycerol mixtures [34] by Puzenko et al. Following their lead, we posit the following, modified Debye formula,

$$\varepsilon^*(\omega) - \varepsilon_\infty = \frac{\Delta\varepsilon \cdot \big(1 + f(\omega)\big)}{1 + i\omega\tau}$$

$$\text{where} \quad f(\omega) = \begin{cases} 0 & \omega < \omega_c \\ A(\omega\tau)^q & \omega \geq \omega_c \end{cases}, \qquad (5)$$

to account for the existence of an excess wing, thermodynamically identified with the main dielectric relaxation peak. Here, ω_c >1/τ is a cut-off frequency, from which the existence of the wing is noticeable, necessary because the Kramers – Kronig relationships [35] for the complex permittivity must be maintained and the modification to the dielectric strength is asymptotic in nature. The parameter *A* controls the amplitude of the excess wing and the exponent *q* is a positive real number. The rationale behind the introduction of an exponent is that to a certain level self-similarity should exist in the timescales for molecular motion in the system. In other words, what happens on the small scale of the molecule should be reflected on the scale of the cluster. This power law dependence indicates that *q* is a fractal dimension of time. The parameters *A* and *q* can further be associated to a new microscopic time scale,

$$A^{1/q} = \frac{\tau_0}{\tau}$$

$$\rightarrow \varepsilon^*(\omega) - \varepsilon_\infty = \frac{\Delta\varepsilon \cdot (1 + (\tau_0\omega)^q)}{1 + i\omega\tau} \qquad \omega > \omega_c, \qquad (6)$$

whereby τ_0 is a new time scale representative of the underlying fast mobilities, responsible for the excess wing. A consequence of the collapse of all temperature spectrums to the same curve in the Master Plot is that the relationship τ_0/τ is constant for all temperatures. Therefore τ_0 possesses the same energy of activation, namely 23 kJmol^{-1}, and so is also linked to the existence of the H-bond network of water. By normalizing equation 6 it can be used to fit the master plots derived from data. Examples of the fits are shown in Figure 4 for the temperature slices 5 °C, 10 °C, 20 °C, 30 °C, 50 and for 70 °C. The averages were calculated for *A* and for *q*, giving *A*=(6.9±0. 2)×10^{-3} and *q*=1.27±0.06, where the standard deviation of the datasets is used as the error estimate.

The implication of A and of q

One may assume that the origin of τ_0 is fast motions on the molecular level. The implication of a power law scaling between it and the overall cluster relaxation time, τ, is that this origin is reflected through the levels of complexity of the cluster structure. From equation 4 this ratio can be calculated, $\tau_0/\tau = A^{1/q} = 0.02$. At 25 °C τ = 8.28 ps [31] and this predicts τ_0=0.17 ps. There are a number of candidates to account for τ_0. At one end of the scale, one is tempted to assign it as the characteristic time for water molecule reorientation in the ELA model. However, this model predicts a characteristic reorientation time of 3 ps [8]. At the other end of the scale, τ_0 is not far from the characteristic time for librations of the water molecule (~ 100 fs)[8]. However, the existence of the master plot collapse implies an energy of activation for τ_0 consistent with the breaking of the H-bond and strong link to the main Debye relaxation time, which is not consistent with the current view of librations [36,37]. The value of τ_0 is close to the predicted proton hopping lifetimes [38,39] in H-bonded structures and that measured in 1h ice [40] and by femtosecond pump probe experiments [41]. While excess protons in pure water from auto-disassociation are necessarily in very low concentrations, the hopping process conceals many rearrangements between different types of protonated water [42] that do not result in a free proton. These rearrangements would lead to a rapid reorganisation of the H-bonded network and the consequent apparent dipole moment of the cluster. This view can be supported by the Molecular Dynamic Simulation (MD) studies by Geissler and Chandler [9] of auto-ionization in water. Their studies produced a number of significant conclusions: 1) that auto-ionization would be the result of a cooperative fluctuation of water molecules, in short a cluster, 2) that the initial transitional state - the separation of the water molecule to H^+ and OH^- ions - would usually terminate to another neutral water molecule within 10 Å and, 3) that the time required for the formation of the intermediate state is 0.15 ps. This time scale coincides with τ_0 as defined above. As their model is essentially a Grotthuss mechanism [43], the dominant energy of activation is the cleavage of an H-bond, related to the motion of the proton through the H-bonded network of water molecules, rather than the dissolving of the O-H bond. They further concluded that there should be an observable signature of this process. A more recent evaluation of this model by Hassanali et al.[44] reveals that the neutralization event – the fast recombination of the Proton and the Hydroxyl ion – does indeed dominate. Using their published distribution of recombination times, one can estimate that recombination events outweigh auto-ionization events by a factor of at least 1000.

The idea of a local fluctuation as initiator of the process has been augmented by MD simulations of the dissociation threshold field for a proton transfer event [45]. This field is about 0.35 V/Å and could exist in the local environment of a water molecule, as a result of neighbouring molecules. While proton transfer due to fluctuating intense local fields is an attractive explanation for the excess wing, the concentration of free protons in pure water is very low. This necessarily demands that within the time scale of cluster reorientation the cascade of proton transfer events should result in an electrically neutral cluster. Simply stated, the starting event leaves an uncompensated

Hydroxyl ion that must recombine with a proton within the characteristic relaxation time of the main dielectric peak (8.28 ps at 25 °C). The stochastic nature of the cascade leaves the apparent dipole moment changed. This scenario is illustrated in figure 5.

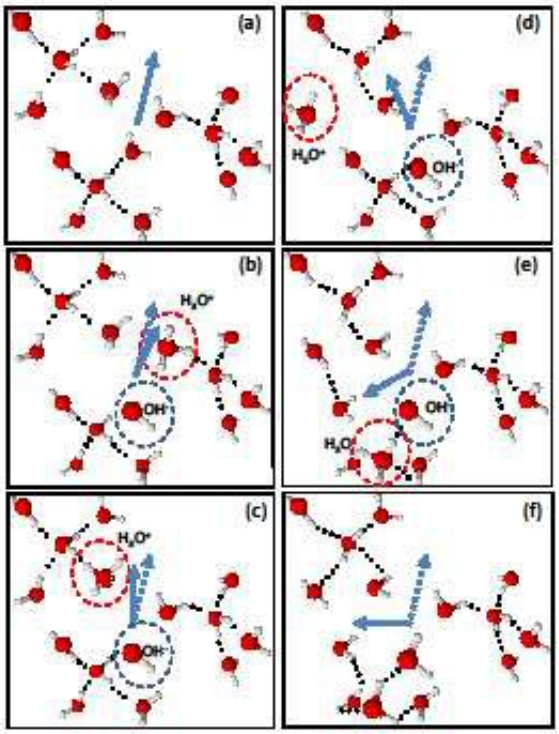

Figure 5 - A schematic illustrating the concept of a proton cascade. The blue arrow in frame (a) represents the apparent dipole moment of the cluster. The dotted lines trace out the H-bond between nearest neighbours. The cascade is initiated by density fluctuations leading to a condition such that local molecular fields are high enough to permit a proton transfer in frame (b), resulting in the formation of a hydronium ion (circled red) and a hydroxyl ion (circled blue). The time scale between frames is in the region of 0.17 ps. The proton migrates though the cluster by the formation of metastable Hydronium (frames (c) to (e)). The last frame (f) represents the closing of the loop as the excess H_3O^+ is neutralized by the uncompensated OH^-. The resulting reorganization of the cluster leads to a change in the apparent dipole moment, represented by the solid blue arrow in frame (f), compared to the dotted blue arrow representing the original dipole moment vector.

Assuming ergodicity, the characteristic time scales can be related to elementary charge movement by the mean square displacement, $\tau \propto R^2$. For the main dielectric peak this implies that the relaxation time will be proportional to the size of the cluster, as dictated by the apparent dipole moment. For the elementary time scale, τ_0, one can assume that it reflects the shortest length scale for the charge motions discussed above, namely the typical length of the hydrogen bond, designated R_0. In this case, the ratio *A* is proportional to the reciprocal of the fractal volume of the elementary water cluster,

$$A^{-1} = \left(\frac{\tau}{\tau_0}\right)^q = G\left(\frac{R}{R_0}\right)^{2q}, \qquad (7)$$

where G is a form factor equal to the ratio of diffusion coefficients for the elementary proton hop and for the diffusion of the apparent dipole moment. The exponent, 2q, would represent the mass fractal dimension, D_S, of the cluster. At 25 °C, $A^{-1} \sim 145$ and this is a measure of the average number of elemental acts required for the reorientation of the apparent dipole moment of the water cluster. This reorientation is the origin of the main dielectric peak.

From the value of q one obtains $D_S \approx 2q = 2.54$. Small Angle Neutron Scattering of aqueous propanol solutions [46] suggest a value of 2.43 for the mass fractal dimension of water clusters., lending credence to the validity of equation 5. If this view is accepted, then one can suppose a distribution of path lengths, $\rho(r)$, for proton transport along the network of H-bond eventually terminating in a recombination with a Hydroxyl ion. Then the characteristic time, τ, for cluster reorientation can be identified as the ensemble averaged time for all transfer events

$$\tau = \langle \tau'(r) \rangle = \int_{\substack{all \\ paths}} dr \rho(r) \tau'(r) \qquad (8)$$

The tail of this distribution, as $r \to \infty$, leads to autoionization. As τ is temperature activated, it follows that $\tau'(r)$ must necessarily be so as well. The consequence of such is that auto-ionization will also demonstrate a strong temperature dependence, a fact well noted [47] (*43*). Furthermore, theoretical ideas of the structure of the water cluster suggest a maximal size of 280 molecules, held together in the form of an icosahedron (*2*). The fractal dimension of such a structure is $D_S = 2.58$ [48](*44*). The collusion of dimensions derived from different methodologies reinforces the interpretation of the excess wing presented here. Certainly, it can no longer be regarded as an independent feature of water relaxation.

It would be tempting to assign the proton cascade as the dominant feature of water's dielectric relaxation. However, to do so would be to ignore the large proportion of water molecules that are not clustered. An analysis of the peak structure associated with the FTIR OH Stretching modes of water reveals that 50 % are not fully coordinated, i.e. clustered [11]. One can assume that the conditions for a local density fluctuation to initiate a proton cascade chain are not common in this population. In this case incidental single molecular, non-cooperative, relaxations will occur. The characteristic time for such events will be similar to those of gaseous water and they would remain most likely indistinguishable from the broad background.

A final consideration one must consider is that if local density fluctuation of the cluster is the initiator of this process then there must be some implications for low frequency Raman Spectroscopy as well. This point is yet to be addressed.

Conclusions

We conclude that there exists a preferential view of the relaxation mechanism of liquid water, one that unifies a number of related phenomena. We account for the existence of auto-ionization as the static limit fast protonic motions that can lead to the rearrangement of the water cluster and the existence of the excess wing in the dielectric spectrum. This model requires no special jump mechanism, but begs to be explored further.

Acknowledgements

The authors would like to thank Profs. Noam Agmon, Dan Huppert, Itamar Procaccia, Valery Ilyin and Dr. Ivan Popov for their fruitful comments and critical discussions. Paul Ben Ishai would like to acknowledge the Matsumae International Foundation for their support of this work.

References

1 B. Bagchi, *Chem. Phys. Lett.*, 2012, **529**, 1–9.
2 M. . Chaplin, *Biophys. Chem.*, 2000, **83**, 211–221.
3 U. Kaatze, *J. Solut. Chem.*, 1997, **26**, 1049–1112.
4 N. Agmon, *J. Phys. Chem.*, 1996, **100**, 1072–1080.
5 N. V. Chekalin and M. I. Shakhparonov, *J. Struct. Chem.*, 1968, **9**, 789–790.
6 D. Laage and J. T. Hynes, *J. Phys. Chem. B*, 2008, **112**, 14230–14242.
7 D. Laage and J. T. Hynes, *Science*, 2006, **311**, 832–835.
8 D. Laage, G. Stirnemann, F. Sterpone, R. Rey and J. T. Hynes, *Annu. Rev. Phys. Chem.*, 2011, **62**, 395–416.
9 P. L. Geissler, C. Dellago, D. Chandler, J. Hutter and M. Parrinello, *Science*, 2001, **291**, 2121–2124.
10 D. Bandyopadhyay, S. Mohan, S. K. Ghosh and N. Choudhury, *J. Phys. Chem. B*, 2013, **117**, 8831–8843.
11 J.-B. Brubach, A. Mermet, A. Filabozzi, A. Gerschel and P. Roy, *J. Chem. Phys.*, 2005, **122**, 184509.
12 Y. Maréchal, *J. Mol. Struct.*, 2011, **1004**, 146–155.
13 C. Huang, K. T. Wikfeldt, T. Tokushima, D. Nordlund, Y. Harada, U. Bergmann, M. Niebuhr, T. M. Weiss, Y. Horikawa, M. Leetmaa, M. P. Ljungberg, O. Takahashi, A. Lenz, L. Ojamäe, A. P. Lyubartsev, S. Shin, L. G. M. Pettersson and A. Nilsson, *Proc. Natl. Acad. Sci.*, 2009, **106**, 15214–15218.

14 J. Vij, D. Simpson and O. Panarina, *J. Mol. Liq.*, 2004, **112**, 125–135.
15 A. A. Chialvo, F. Moucka, L. Vlcek and I. Nezbeda, *J. Phys. Chem. B*, 2015, **119**, 5010–5019.
16 D. D. Kemp and M. S. Gordon, *J. Phys. Chem. A*, 2008, **112**, 4885–4894.
17 A. V. Gubskaya and P. G. Kusalik, *J. Chem. Phys.*, 2002, **117**, 5290–5302.
18 A. R. von Hippel, *IEEE Trans. Electr. Insul.*, 1988, **23**, 801–816.
19 H. Frohlich, *Theory of Dielectrics: Dielectric Constant and Dielectric Loss*, Oxford University Press, USA, 2nd edn., 1987.
20 R. Buchner, J. Barthel and J. Stauber, *Chem. Phys. Lett.*, 1999, **306**, 57–63.
21 C. Rønne, L. Thrane, P.-O. Åstrand, A. Wallqvist, K. V. Mikkelsen and S. R. Keiding, *J. Chem. Phys.*, 1997, **107**, 5319–5331.
22 W. T. Coffey, Y. P. Kalmykov and S. V. Titov, in *Fractals, Diffusion, and Relaxation in Disordered Complex Systems*, eds. W. T. Coffey and Y. P. Kalmykov, John Wiley & Sons, Inc., 2006, pp. 285–437.
23 H. B. Ke, P. Wen and W. H. Wang, *ArXiv11114608 Cond-Mat Physicsphysics*, 2011.
24 Y. Wang, M. Zhang, A. S. Mujumdar and K. J. Mothibe, *Dry. Technol.*, 2012, **30**, 1377–1386.
25 L. R. Winther, J. Qvist and B. Halle, *J. Phys. Chem. B*, 2012, **116**, 9196–9207.
26 T. Sato and R. Buchner, *J. Mol. Liq.*, 2005, **117**, 23–31.
27 I. Bakó, A. Bencsura, K. Hermannson, S. Bálint, T. Grósz, V. Chihaia and J. Oláh, *Phys. Chem. Chem. Phys. PCCP*, 2013, **15**, 15163–15171.
28 L. B. Pártay, P. Jedlovszky, I. Brovchenko and A. Oleinikova, *Phys. Chem. Chem. Phys.*, 2007, **9**, 1341–1346.
29 C. Rønne and S. R. Keiding, *J. Mol. Liq.*, 2002, **101**, 199–218.
30 H. Hirori, K. Yamashita, M. Nagai and K. Tanaka, *Jpn. J. Appl. Phys.*, 2004, **43**, L1287–L1289.
31 W. J. Ellison, *J. Phys. Chem. Ref. Data*, 2007, **36**, 1–18.
32 W. J. Ellison, K. Lamkaouchi and J.-M. Moreau, *J. Mol. Liq.*, 1996, **68**, 171–279.
33 P. U. Jepsen and H. Merbold, *J. Infrared Millim. Terahertz Waves*, 2009.
34 A. Puzenko, Y. Hayashi, Y. E. Ryabov, I. Balin, Y. Feldman, U. Kaatze and R. Behrends, *J. Phys. Chem. B*, 2005, **109**, 6031–6035.
35 F. Kremer and A. Schönhals, *Broadband Dielectric Spectroscopy*, Springer, 1st edn., 2002.
36 F. Ingrosso, R. Rey, T. Elsaesser and J. T. Hynes, *J. Phys. Chem. A*, 2009, **113**, 6657–6665.
37 H. R. Zelsmann, *J. Mol. Struct.*, 1995, **350**, 95–114.
38 V. Krasnoholovets, P. Tomchuk and S. lukyanets, in *Advances in Chemical Physics,* John Wiley & Sons Inc., 2003, vol. 125, pp. 351–548.
39 N. Uddin, J. Kim, B. J. Sung, T. H. Choi, C. H. Choi and H. Kang, *J. Phys. Chem. B*, 2014, **118**, 13671–13678.
40 I. Presiado, J. Lal, E. Mamontov, A. I. Kolesnikov and D. Huppert, *J. Phys. Chem. C*, 2011, **115**, 10245–10251.
41 S. Woutersen and H. Bakker, *Phys. Rev. Lett.*, 2006, **96**, 138305.
42 H. Lapid, N. Agmon, M. K. Petersen and G. A. Voth, *J. Chem. Phys.*, 2004, **122**, 014506–014506–11.
43 N. Agmon, *Chem. Phys. Lett.*, 1995, **244**, 456–462.
44 A. Hassanali, M. K. Prakash, H. Eshet and M. Parrinello, *Proc. Natl. Acad. Sci.*, 2011, **108**, 20410–20415.
45 A. M. Saitta, F. Saija and P. V. Giaquinta, *Phys. Rev. Lett.*, 2012, **108**, 207801.
46 M. Misawa, I. Dairoku, A. Honma, Y. Yamada, T. Sato, K. Maruyama, K. Mori, S. Suzuki and T. Otomo, *J. Chem. Phys.*, 2004, **121**, 4716–4723.
47 J. W. Moore, C. L. Stanitski and P. C. Jurs, *Chemistry: The Molecular Science, Volume II, Chapters 12-22*, Cengage Learning, Princeton, N.J., 3 edition., 2007.
48 B. K. Teo and H. Zhang, *J. Clust. Sci.*, 1995, **6**, 203–215.